Polarity establishment requires localized activation of Cdc42

Benjamin Woods, Chun-Chen Kuo, Chi-Fang Wu, Trevin R. Zyla, and Daniel J. Lew

Department of Pharmacology and Cancer Biology, Duke University Medical Center, Durham, NC 27710

Establishment of cell polarity in animal and fungal cells involves localization of the conserved Rho-family guanosine triphosphatase, Cdc42, to the cortical region destined to become the "front" of the cell. The high local concentration of active Cdc42 promotes cytoskeletal polarization through various effectors. Cdc42 accumulation at the front is thought to involve positive feedback, and studies in the budding yeast *Saccharomyces cerevisiae* have suggested distinct positive feedback mechanisms. One class of mechanisms involves localized activation of Cdc42 at the front, whereas another class involves localized delivery of Cdc42 to the front. Here we show that Cdc42 activation must be localized for successful polarity establishment, supporting local activation rather than local delivery as the dominant mechanism in this system.

Introduction

The Rho-family GTPase, Cdc42, and its relatives are master regulators of cell polarity in most eukaryotes (Etienne-Manneville, 2004; Park and Bi, 2007; Wu et al., 2013). During polarity establishment, cells concentrate GTP-Cdc42 at a site on the cortex that then becomes the front of the cell (Ziman et al., 1993; Gulli et al., 2000). In budding yeast, there is consensus that polarity establishment involves positive feedback that can amplify small initial asymmetries in Cdc42 distribution to generate a highly concentrated patch of Cdc42. However, the mechanisms of positive feedback remain controversial.

Models of positive feedback via "local activation" posit that GTP-Cdc42 promotes GTP loading of neighboring GDP-Cdc42 at the plasma membrane by recruiting the guanine nucleotide exchange factor (GEF) Cdc24 (Goryachev and Pokhilko, 2008; Kozubowski et al., 2008; Johnson et al., 2011). Consistent with local activation, Cdc24 becomes co-concentrated with GTP-Cdc42 at the polarity site (Nern and Arkowitz, 1999; Toenjes et al., 1999). On the other hand, "local delivery" models posit that GTP-Cdc42 promotes targeted delivery of more Cdc42 (GDP or GTP bound) to the local vicinity from internal pools (Wedlich-Soldner et al., 2003; Slaughter et al., 2009, 2013). Local activation and local delivery are not mutually exclusive. However, findings from different laboratories have led to contradictory conclusions about their relative importance.

Support for the local activation model came from analyses of two proteins, Rsr1 and Bem1, which bind Cdc24 and concentrate it at the polarity site. Rsr1 is a Ras-family GTPase activated in the vicinity of "landmark" proteins inherited at specific sites by newborn cells. Rsr1-GTP can recruit Cdc24 from the cytoplasm, leading to Cdc42 activation near the landmarks (Howell and Lew, 2012). Bem1 is a scaffold protein that binds Cdc42-GTP and Cdc42 effectors in addition to Cdc24. These interactions allow GTP-Cdc42 to recruit Bem1-Cdc24 complexes from the cytoplasm, leading to GTP loading of neighboring Cdc42 in a positive feedback loop (Goryachev and Pokhilko, 2008; Kozubowski et al., 2008; Johnson et al., 2011). Cells lacking Rsr1 or Bem1 can polarize Cdc42, but cells lacking both cannot (Irazoqui et al., 2003). As Rsr1 and Bem1 act to localize Cdc24, these findings suggested that Cdc24 localization, and hence local activation of Cdc42, was critical for polarization.

A recent study (Smith et al., 2013) suggested that Rsr1-Cdc24 and Bem1-Cdc24 interactions are important primarily to activate Cdc24, not to localize it. In this view, Rsr1 and Bem1 simply enable sufficient GTP loading of Cdc42 to trigger positive feedback by local delivery: Localization of Cdc24 is not necessary, and as long as there is sufficient GEF activity it does not matter where the GTP loading of Cdc42 takes place. Here, we have directly tested this hypothesis. We demonstrate that local activation of Cdc42 is a key event in polarity establishment.

Results and discussion

Can polarization occur without *RSR1* and *BEM1*?

We previously reported that *rsr1*Δ *bem1*Δ mutants were inviable in three different strain backgrounds, including S288C (Irazoqui et al., 2003). However, Smith et al. (2013) found that at 24°C, *rsr1*Δ *bem1*Δ mutants were viable in their version of S288C. By dissecting tetrads from diploid strains provided

Correspondence to Daniel J. Lew: daniel.lew@duke.edu

Abbreviations used in this paper: CCD, charge-coupled device; CSM, complete synthetic medium; dex, dextrose; DIC, differential interference contrast; FRB, FKBP12-rapamycin–binding; GEF, guanine nucleotide exchange factor; MT, membrane-targeted; YEP, yeast extract Bacto peptone.

The Rockefeller University Press $30.00
J. Cell Biol. Vol. 211 No. 1 19–26
www.jcb.org/cgi/doi/10.1083/jcb.201506108

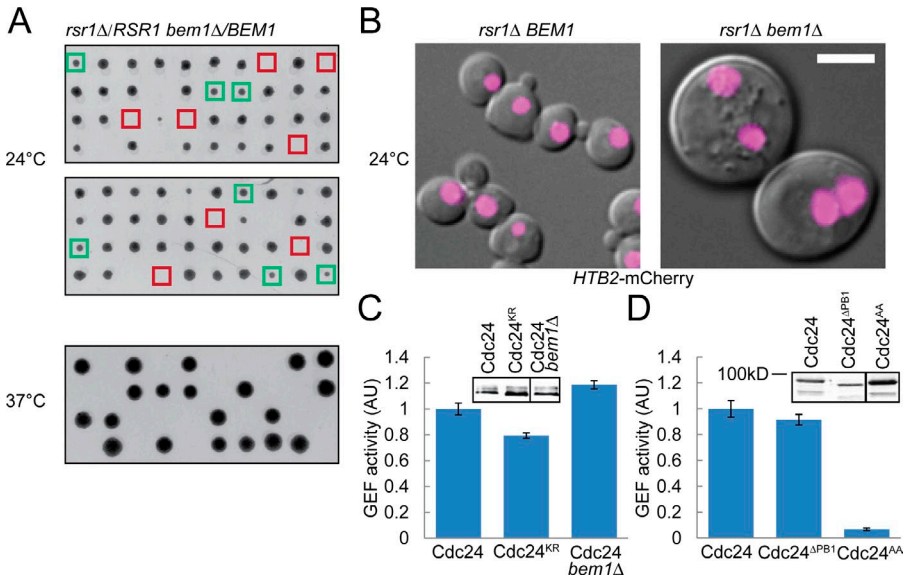

Figure 1. **Requirement for *BEM1* and *RSR1* and biochemical assay of the effect of Bem1 on Cdc24 GEF activity.** (A) Tetrads from *rsr1Δ/RSR1 bem1Δ/BEM1* S288C diploids (DLY17480). *rsr1Δ bem1Δ* spores often fail to produce viable colonies at 24°C. Green, viable *rsr1Δ bem1Δ* spores; red, inviable *rsr1Δ bem1Δ* spores. At 37°C, both *RSR1 bem1Δ* and *rsr1Δ bem1Δ* spores are inviable. (B) DIC images of *rsr1Δ BEM1* and viable *rsr1Δ bem1Δ* cells (DLY18495 and DLY18459) expressing the histone H2B tagged with mCherry. These cells were generated from a transformed diploid strain constructed by using haploids isolated from the tetrads in A. Scale bar, 5 µm. (C and D) Cdc24 GEF activity in vitro. Arbitrary units (AU): amount of radioactive GTP loaded on Cdc42 divided by the amount of HA-Cdc24 in the immunoprecipitate (inset). Activity is normalized to the wild-type Cdc24. (C) Cdc42 GTP loading by Cdc24 isolated from yeast: wild-type, DLY15284; $Cdc24^{KR}$ (no Bem1 binding), DLY17327; Cdc24 from *bem1Δ* cells, DLY15299. (D) Wild-type, DLY15819; $Cdc24^{\Delta PB1}$ (lacks putative autoinhibition), DLY15818; $Cdc24^{AA}$ (catalytically dead control), DLY15817. Mean ± SEM ($n = 3$).

by S. Smith and R. Li (Johns Hopkins University School of Medicine, Baltimore, MD), we found that most *rsr1Δ bem1Δ* spores failed to yield viable colonies even at 24°C (Fig. 1 A); those that did contained many abnormally large and multinucleate cells (Fig. 1 B and Fig. S1). These data do support the existence of a mechanism that can drive bud emergence without Bem1 and Rsr1, whose nature remains to be determined. However, the process is clearly too weak to support polarization in a majority of cells.

Is Cdc24 activated by Bem1?

A membrane-targeted (MT) FRET-based Cdc42 biosensor reported higher GTP-Cdc42 levels in wild-type cells than in *bem1Δ* cells or *bem1* point mutants that disrupt the Bem1-Cdc24 interaction (Smith et al., 2013), prompting the conclusion that Bem1–Cdc24 interaction stimulates Cdc24 GEF activity. However, because Bem1–Cdc24 interaction localizes Cdc24 to the polarity site at the cell cortex, that alone would increase access of Cdc24 to the membrane-localized Cdc42, enhancing overall GTP loading of Cdc42.

To ask whether Cdc24 activity is regulated by Bem1 interaction, we isolated Cdc24 from wild-type and *bem1Δ* mutant strains and compared its GEF activity in vitro. Both preparations were active (Fig. 1 C). Indirect experiments had suggested that the PB1 domain of Cdc24 was autoinhibitory and that Bem1 binding to that domain activated Cdc24 by relief of autoinhibition (Shimada et al., 2004). However, disrupting the Bem1-Cdc24 interaction by point mutation (Fig. 1 C) or deleting the PB1 domain (Fig. 1 D) had little effect on Cdc24 GEF activity. Because in vitro assays may not recapitulate in vivo conditions, it remains possible that Bem1 regulates Cdc24 catalytic activity. However, this hypothesis lacks direct support in a context that distinguishes catalytic activity from membrane targeting.

Bem1 polarization is necessary for Bem1 function

Whether or not Bem1 activates Cdc24, a key prediction of the local activation model is that Bem1 must concentrate at the polarity site to function. A mutant with reduced binding to GTP-Cdc42 ($Bem1^{N253D}$) was still able to promote Cdc42 polarization (Smith et al., 2013), but previous work suggested that Bem1 localization occurs primarily via the second SH3 domain, which binds effectors of Cdc42 (Irazoqui et al., 2003; Kozubowski et al., 2008). Indeed, $Bem1^{N253D}$-GFP polarized with similar timing to wild-type Bem1-GFP (Fig. 2 A), so the ability of $Bem1^{N253D}$ to function is unsurprising.

To determine whether Bem1 localization was necessary for Bem1 function, we exploited the chemical genetic "anchor away" system (Haruki et al., 2008) to generate a version of Bem1 that could be trapped in the cytoplasm (Fig. 2 B). In this system, rapamycin promotes interaction of Bem1 with ribosomes, rapidly sequestering Bem1 away from the polarity site (Fig. 2 C). Addition of rapamycin blocked bud emergence (Fig. 2 D and Video 1), indicating that Bem1 cannot function in the cytoplasm. Interestingly, this was true even in cells that contain Rsr1, where Bem1 itself is nonessential (Fig. S2). Our results are fully consistent with recent findings that optogenetic sequestration of Bem1 to the surface of mitochondria similarly blocked bud emergence (Jost and Weiner, 2015). Thus, Bem1 must be able to localize to the cortex to function.

To test whether Bem1 must concentrate at the polarity site or whether general membrane localization would suffice, we exploited previously characterized constructs in which Bem1 is fused to the transmembrane protein Snc2 (Howell et al., 2009). Snc2 is a v-SNARE that becomes polarized by delivery on exocytic vesicles and rapid endocytic recycling (Valdez-Taubas and Pelham, 2003). We showed that Bem1-Snc2 polarized like Snc2 and was able to promote budding (Howell et al., 2009). However, mutation of the Snc2 endocytosis signal caused Bem1-$Snc2^{V39A,M42A}$ to localize patchily all over the plasma membrane (Fig. 2 E). Introducing this construct into the anchor-away strain, we found that Bem1-$Snc2^{V39A,M42A}$ could not rescue budding upon addition of rapamycin (Fig. 2 F and Video 2). We conclude that general membrane localization of Bem1 cannot promote polarization, and that Bem1 polarization is essential for Bem1 function.

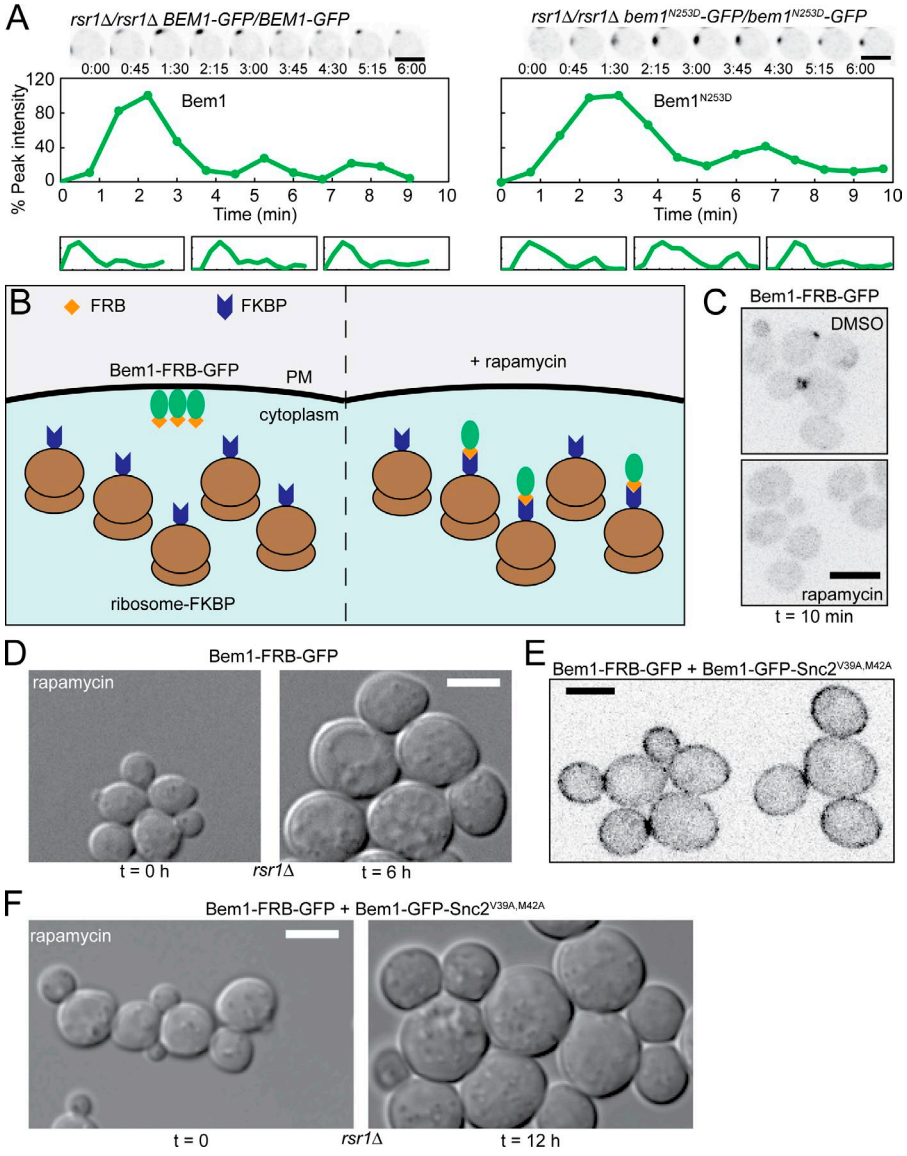

Figure 2. **Bem1 localization is necessary for Bem1 function.** (A) Wild-type Bem1 and a Cdc42 interaction–defective mutant (Bem1^{N253D}) polarize with similar dynamics. Top: Inverted maximum projection images at 45-s intervals comparing Bem1-GFP and Bem1^{N253D}-GFP homozygous diploids (DLY17251 and DLY19400). Time point starting just before polarization. Middle: Quantification of Bem1-GFP or Bem1^{N253D}-GFP cluster intensity in the cells above. Bottom: Additional quantifications of different cells. (B) Anchor-away technique: FRB (orange diamond) and GFP are fused to the C terminus of Bem1, and the FKBP12 domain (blue arrow) is fused to the C terminus of the large ribosomal subunit Rpl13a. In the absence of rapamycin, Bem1 localizes normally to the polarity site (left). In the presence of rapamycin, FKBP12 and FRB interact, sequestering Bem1 to the ribosomes (right). PM, plasma membrane. (C) Sequestering Bem1 to ribosomes blocks Bem1 polarization. Upon addition of rapamycin, Bem1-FRB-GFP is sequestered to the cytoplasm. Inverted, maximum projection images of cells (DLY15549) expressing Bem1-FRB in DMSO or 50 µg/ml rapamycin. (D) Sequestering Bem1 to the cytoplasm blocks budding. DIC images of *rsr1*Δ cells expressing Bem1-FRB-GFP (DLY15971) before and after 6-h incubation on a 50-µg/ml rapamycin slab. See Video 1. (E) Bem1 fused to a plasma membrane protein (Snc2^{V39A,M42A}) localizes to the plasma membrane. Inverted single-slice-scanning confocal image of diploid cells expressing Bem1-GFP-FRB and Bem1-GFP-Snc2^{V39A,M42A} (DLY18783). (F) Localization of Bem1 to the plasma membrane does not rescue budding. DIC images of cells expressing Bem1-FRB-GFP and Bem1-GFP-Snc2^{V39A,M42A} (DLY19244) before and after 12-h incubation on a 50-µg/ml rapamycin slab. See Video 2. Bars, 5 µm.

Cdc24 polarization is necessary for Cdc24 function

A delocalized version of Cdc24 lacking the C-terminal PB1 domain, Cdc24$^{\Delta PB1}$, was reported to promote Cdc42 biosensor activation and perhaps aid in Cdc42 polarization, even though it could not bind Bem1 or concentrate at the polarity site (Smith et al., 2013). However, in agreement with earlier work (Kozubowski et al., 2008), we found that Cdc24$^{\Delta PB1}$ was unable to sustain viability in the absence of endogenous Cdc24 (Fig. 3 A), suggesting that delocalized Cdc24 is not functional.

Cdc24$^{\Delta PB1}$ is primarily cytoplasmic, whereas its target, Cdc42, is associated with membranes. Thus, the inability of Cdc24$^{\Delta PB1}$ to function may simply reflect lack of access to the plasma membrane. To test this possibility, we fused Cdc24$^{\Delta PB1}$ (or full-length Cdc24 as control) to a 28-residue N-terminal peptide from Psr1, which confers plasma membrane localization via myristoylation and dual palmitoylation (Siniossoglou et al., 2000; Kuo et al., 2014). We refer to these as MT versions. Because previous experiments indicated that Cdc24 undergoes inhibitory phosphorylation at the plasma membrane (Kuo et al., 2014), we also generated versions that were nonphosphorylatable and hence could not be inhibited: MT-Cdc24^{38A} and MT-Cdc24$^{37A\ \Delta PB1}$. These proteins were expressed (Fig. 3 B) and targeted to the plasma membrane (Fig. 3 C), but MT-Cdc24^{38A} was polarized whereas MT-Cdc24$^{37A\ \Delta PB1}$ was not. MT-Cdc24^{38A} rescued the viability of *cdc24*Δ mutants, but MT-Cdc24$^{37A\ \Delta PB1}$ did not (Fig. 3 D). In a temperature-sensitive *cdc24-1* context, cells expressing MT-Cdc24^{38A} polarized and budded, but cells expressing MT-Cdc24$^{37A\ \Delta PB1}$ arrested as large, round, unbudded cells at restrictive temperature (Fig. 3, E and F; and Video 3). Indeed, these cells were large even at permissive temperature, suggesting that unpolarized, active Cdc24$^{37A\ \Delta PB1}$ interferes with polarization. Similar results were obtained with MT-Cdc24 and MT-Cdc24$^{\Delta PB1}$ (Fig. S3). Thus, uniformly targeting Cdc24 to the plasma membrane is not sufficient to promote polarization, suggesting that localizing GEF activity is essential.

A remaining caveat is that truncation of the PB1 domain might render Cdc24 nonfunctional for reasons other than its localization. We consider this unlikely because Cdc24$^{\Delta PB1}$ retained normal GEF activity in vitro (Fig. 1 D). However, as an additional test, we generated a Cdc24$^{37A\ \Delta PB1}$-Snc2 fusion analogous to the Bem1-Snc2 fusions discussed earlier. Fusion to Snc2 restored polarization (Fig. 4 A) and function to the oth-

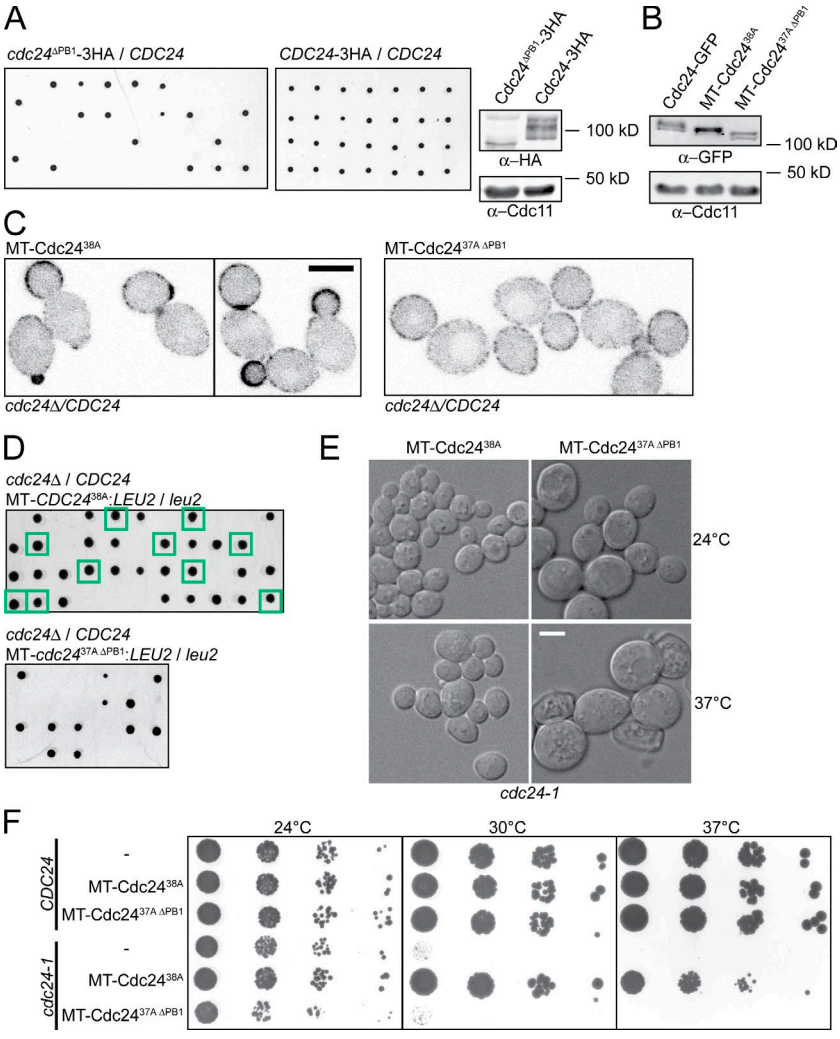

Figure 3. **Cdc24 localization is necessary for Cdc24 function.** (A) Cdc24$^{\Delta PB1}$ is unable to function as the sole source of Cdc24. Left: Tetrads of heterozygous diploids expressing Cdc24$^{\Delta PB1}$-3HA (DLY15184) or Cdc24-3HA (DLY15073) at the *CDC24* locus were grown at 24°C for 2 d. (right) Western blot of Cdc24 from the heterozygous diploids. (B) Western blot comparing expression of nonphosphorylatable, membrane-targeted MT-Cdc24^{38A} (DLY18203) and MT-Cdc24$^{37A\ \Delta PB1}$ (DLY18490) relative to wild-type Cdc24 (DLY12338). (C) MT-Cdc24 localizes to the plasma membrane. Inverted single-slice-scanning confocal image of heterozygous diploid cells expressing MT-Cdc24^{38A} (DLY18203) or MT-Cdc24$^{37A\ \Delta PB1}$ (DLY18490). Bar, 5 µm. (D) MT Cdc24$^{37A\ \Delta PB1}$ is unable to function as the sole source of Cdc24. Tetrads of heterozygous *cdc24Δ/CDC24* diploids expressing MT-Cdc24^{38A} (DLY18203) or MT-Cdc24$^{37A\ \Delta PB1}$ (DLY18490) were grown at 24°C for 3 d. Green boxes indicate viable *cdc24Δ* colonies, showing rescue by MT-Cdc24^{38A}. (E) MT Cdc24$^{37A\ \Delta PB1}$ causes arrest as large, round, unbudded cells. DIC images of *cdc24-1* cells expressing MT-Cdc24^{38A} (DLY19120) or MT-Cdc24$^{37A\ \Delta PB1}$ (DLY19218) shifted to 37°C for 6 h. Bar, 5 µm. (F) MT Cdc24$^{37A\ \Delta PB1}$ is unable to rescue *cdc24-1*. Cells were spotted onto plates (10-fold serial dilutions) and incubated for 3 d. From top: DLY8502, DLY19122, DLY19498, DLY8534, DLY19120, and DLY19218.

erwise nonfunctional Cdc24$^{37A\ \Delta PB1}$: cells containing this construct as the sole source of Cdc24 proliferated successfully (Fig. 4 B). Similarly, fusion of Cdc24$^{\Delta PB1}$ to the Cdc42 effector Cla4 (a p21-activated kinase) or to the SH3-2 domain of Bem1 (which binds to Cla4 and other Cdc42 effectors) restored both localization and function to Cdc24$^{\Delta PB1}$ (Kozubowski et al., 2008). Thus, the functional deficit of a Cdc24 that lacks the PB1 domain can be rescued by linkage to a polarized protein, whether that protein polarizes by diffusion capture (Cla4) or vesicle recycling (Snc2).

As discussed earlier, Bem1-Snc2 was able to rescue polarization in *rsr1*Δ *bem1*Δ cells, even though the fusion protein was polarized by a vesicular mechanism. We showed previously that such "re-wired" cells used an artificial positive feedback mechanism to polarize and occasionally generate two buds at the same time (Howell et al., 2009). If the only essential role for Bem1 and Rsr1 is to localize Cdc24 to the polarity site, then cells containing Cdc24-Snc2 derivatives (which also polarize by a vesicular mechanism) should no longer require Bem1 or Rsr1. Indeed, cells containing Cdc24^{38A}-Snc2 or Cdc24$^{37A\ \Delta PB1}$-Snc2 as the sole source of Cdc24 could polarize (Fig. S3) and proliferate in the absence of Rsr1 and Bem1 (Fig. 4 C). As with Bem1-Snc2, occasional cells had two buds (Fig. S3). The finding that heterologous localization of Cdc24 (with or without the PB1 domain) to the polarity site rescues *rsr1*Δ *bem1*Δ synthetic lethality indicates that the essential role of Bem1 and Rsr1 is to localize the GEF.

Previous studies showed that overexpression of MT-Cdc24 blocked polarization even if cells also had an endogenous wild-type Cdc24 (Shimada et al., 2004; Kuo et al., 2014). Unlike MT-Cdc24 expressed at endogenous levels, which became concentrated at the polarity site (Fig. 3 C), overexpressed MT-Cdc24 accumulated uniformly all over the membrane (Kuo et al., 2014). The dominant lethality of overexpressed MT-Cdc24 could be due to excessive Cdc42 activation or to a lack of localized GTP loading of Cdc42. Co-overexpression of Bem1 rescued the lethality of overexpressed MT-Cdc24 (Fig. 4 D), allowing cells to bud and in many cases to concentrate MT-Cdc24 in the bud (Fig. 4 E). This result is not consistent with the view that lethality is attributable to excess GTP-Cdc42 because extra Bem1 should (if anything) increase GTP loading even further. Instead, we conclude that the lethality of overexpressed MT-Cdc24 stems from the failure to localize GTP loading of Cdc42. The effect is dominant because the overexpressed MT-Cdc24 titrates Bem1 away from the endogenous Cdc24, but that can be ameliorated by co-overexpression of Bem1. In summary, our findings show that blocking Cdc24 accumulation at the polarity site by any of several strategies (deletion of the PB1 domain, blocking Bem1 localization, or overexpression of MT-Cdc24) blocks polarization and budding.

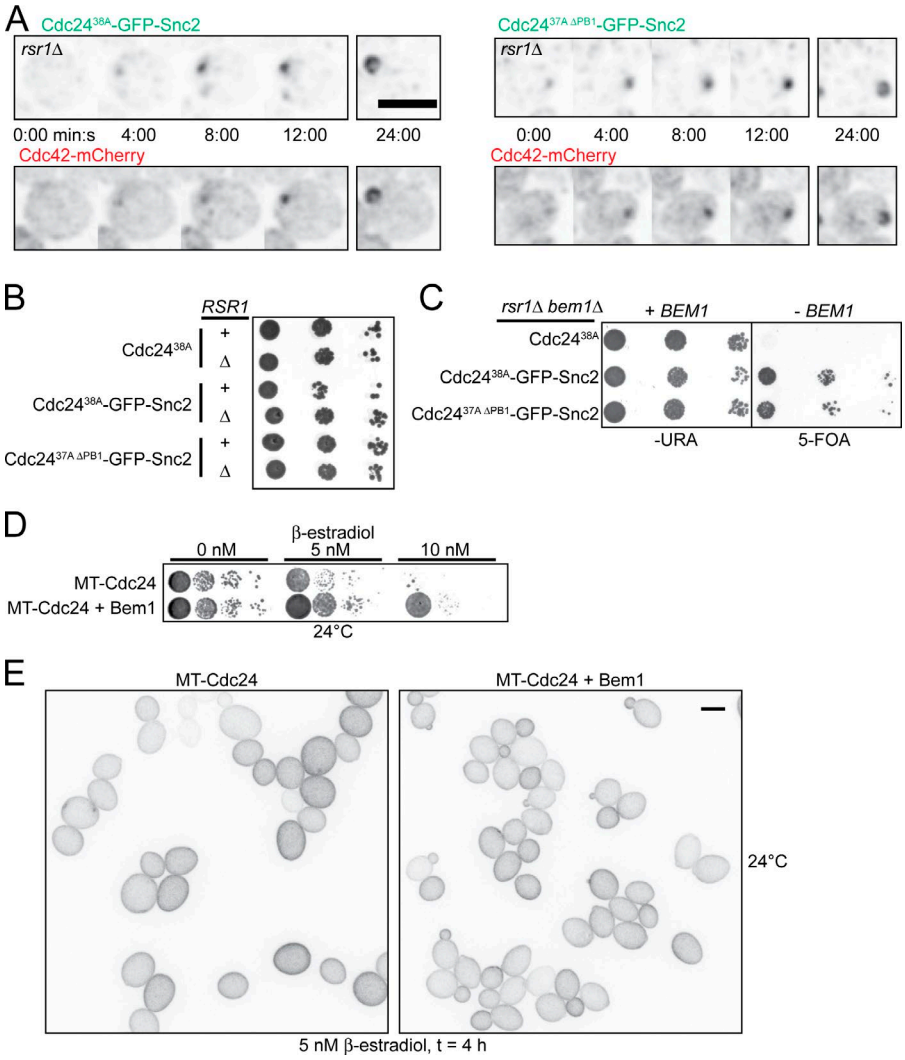

Figure 4. **Heterologous localization of Cdc24$^{\Delta PB1}$ restores function.** (A) Cdc24^{38A}-Snc2 and Cdc24$^{37A\ \Delta PB1}$-Snc2 polarize together with Cdc42. Inverted, maximum projection images from a time lapse of cells expressing Cdc42-mCherry^{SW} and either Cdc24^{38A} or Cdc24$^{37A\ \Delta PB1}$ fused to GFP-Snc2 (Cdc24^{38A}-Snc2, DLY19558; Cdc24$^{37A\ \Delta PB1}$-Snc2, DLY19560). Time in minutes, starting just before cells begin to polarize. Bar, 5 µm. (B) Cdc24^{38A}-Snc2 and Cdc24$^{37A\ \Delta PB1}$-Snc2 are functional as the sole source of Cdc24. Wild-type and *rsr1*Δ cells with the indicated Cdc24 construct at the endogenous locus were spotted (10-fold serial dilutions) and incubated for 2 d at 30°C. From top: DLY17405, DLY17402, DLY19606, DLY19604, DLY18430, and DLY18603. (C) Heterologous polarization of Cdc24 bypasses the need for Rsr1 and Bem1 in polarity establishment. *rsr1*Δ *bem1*Δ cells containing the indicated Cdc24-Snc2 fusions as the only source of Cdc24 and carrying a *URA3*-marked *BEM1* plasmid were grown to mid-log phase, spotted (10^4, 10^3, and 10^2 cells) onto medium with or without 5-fluoroorotic acid (to select for plasmid loss), and incubated for 2 d at 30°C. From top: DLY19826, DLY19773, and DLY19774. (D) Overexpression of Bem1 rescues the lethality of MT-Cdc24 overexpression. Cells were spotted onto plates containing the indicated concentrations of β-estradiol to induce overexpression of MT-Cdc24 alone (DLY15297) or MT-Cdc24 and Bem1 (DLY15311) and incubated for 2 d at 24°C. (E) Overexpression of Bem1 restores budding to cells overexpressing MT-Cdc24. Inverted, maximum projection images of cells incubated for 4 h in 5 nM β-estradiol medium to induce overexpression of MT-Cdc24 alone (DLY15297) or MT-Cdc24 and Bem1 (DLY15311). MT-Cdc24 itself becomes enriched in most buds of cells coexpressing Bem1. Bar, 5 µm.

Conclusions

A key requirement of the local activation model is that GEF activity be targeted to the polarity site. Here we show that delocalized Cdc24 GEF activity is unable to support polarization. A major pathway for localizing Cdc24 is mediated by interaction with Bem1, and we found that, as for Cdc24, localization of Bem1 was essential for polarization. The finding that Bem1 and Cdc24 must polarize to function supports the local activation model in which localized GTP loading of Cdc42 underlies polarity establishment.

Our findings do not rule out the possibility that Cdc42 is also delivered to the polarity site. Indeed, a recent study suggested that Cdc42 undergoes endocytosis and recycling to the cortex on secretory vesicles (Watson et al., 2014). However, the Cdc42 concentration on secretory vesicles was estimated to be approximately threefold lower than that at the polarity site (Watson et al., 2014). Thus, as predicted by modeling studies (Layton et al., 2011; Savage et al., 2012), vesicles would dilute Cdc42 at the polarity site rather than concentrating it. Our findings indicate that localized delivery of Cdc42 is insufficient for polarization in the absence of localized Cdc42 activation.

If not through localized delivery, how does Cdc42 itself become concentrated at the polarity site? If GDP-Cdc42 has a higher mobility than GTP-Cdc42, then when fast-moving GDP-Cdc42 gets converted to slow-moving GTP-Cdc42 at the polarity site, local activation will result in local enrichment of total Cdc42. Guanine nucleotide dissociation inhibitors selectively bind to GDP-Cdc42 (Johnson et al., 2009) and increase its mobility by facilitating transfer from the membrane to the cytoplasm. When combined with Bem1-mediated localization of Cdc24, this would suffice to enable dramatic concentration of Cdc42 at the polarity site (Goryachev and Pokhilko, 2008; Johnson et al., 2011). In the distantly related fission yeast *Schizosaccharomyces pombe*, GDP-Cdc42 diffuses much more rapidly than GTP-Cdc42 at the plasma membrane (Bendezú et al., 2015). As with the cytoplasmic mobilization pathway in budding yeast, this also enabled Cdc42 enrichment in response to local activation.

Our findings demonstrate that local activation of Cdc42 is necessary for polarization in budding yeast. Given the differential mobility of GDP-Cdc42 and GTP-Cdc42, local activation may also be sufficient to explain polarization without need for directed delivery.

Materials and methods

Yeast strains

Yeast strains used in this study are listed in Table S1. Experiments assessing the function of Bem1 derivatives were performed in strains

lacking *RSR1*. The polarity markers *BEM1*-GFP (Kozubowski et al., 2008), *SPA2*-mCherry (Longtine et al., 1998), *ABP1*-mCherry (Howell et al., 2009), *CDC24*-GFP, and *BEM1*-tdTomato (Howell et al., 2012), replacing endogenous genes, are functional as previously described. *HTB2*-mCherry (gift from K. Bloom) was amplified from genomic DNA and integrated at the endogenous locus. Functional GFP-*SEC4* (Chen et al., 2012) was integrated at the *URA3* locus as previously described. *CDC42*-mCherry^{SW} was based on the Cdc42 probe first reported in *S. pombe* (Bendezú et al., 2015), and integrated at the *URA3* locus. To generate Cdc24^{38A}-GFP-Snc2 or Cdc24$^{37A\ \Delta PB1}$-GFP-Snc2, we constructed a new vector based on the PCR-based C-terminal tagging method (Longtine et al., 1998). *BEM1*-GFP-*SNC2*^{V39A,M42A} (Howell et al., 2009) was integrated at the *URA3* locus as previously described.

To replace the endogenous *BEM1* with *bem1*^{N253D}-GFP, we deleted one copy of *BEM1* in a diploid strain with *URA3*. An integrating *bem1*^{N253D}-GFP:*TRP1* plasmid (DLB4214) was constructed by subcloning the 1.8 kbp SmaI–XcmI fragment containing the N253D mutation from pSAS014 (gift from S. Smith and R. Li) into the *BEM1*-GFP plasmid DLB2997. Integration was targeted to the *BEM1* promoter by digestion with SmaI. We selected transformants that integrated *bem1*^{N253D}-GFP next to *bem1*::*URA3*.

To generate MT-Cdc24^{38A} and MT-Cdc24$^{37A\ \Delta PB1}$, we appended the codons encoding first 28 residues from *PSR1* to the N terminus of the GFP-*CDC24*^{38A} and GFP-*CDC24*$^{37A\ \Delta PB1}$, respectively (Siniossoglou et al., 2000; Kuo et al., 2014). For endogenous or near-endogenous expression, these were integrated at the *LEU2* locus under control of the *CDC24* promoter. Overexpression of MT-Cdc24 was controlled by a β-estradiol inducible *GAL1* promoter (Takahashi and Pryciak, 2008).

To generate overexpressed HA-tagged Cdc24 for biochemical assays, we used one of two strategies: a high-copy 2-µm YEPlac195 plasmid (Gietz and Sugino, 1988) with the *ADH1* promoter driving expression, or a *GAL1* promoter driving expression from the endogenous locus (Kuo et al., 2014). Additionally, a derivative of HA-taggedCdc24 expressed from YEPlac195 was constructed, which harbored mutations D824K and D831R in the PB1 domain (Cdc24^{KR}; Ito et al., 2001). A derivative of HA-tagged Cdc24 expressed behind the *GAL1* promoter at the endogenous locus, which harbored mutations N452A and E453A, was constructed as described previously (Kuo et al., 2014). A derivative of HA-tagged Cdc24 lacking the PB1 domain behind the *GAL1* promoter at the endogenous locus was constructed using the PCR-based C-terminal tagging method (Longtine et al., 1998).

Rapamycin experiments were performed in *TOR1-1 fpr1*Δ strains as described (Haruki et al., 2008). To use the ribosome "anchor," two tandem copies of FKBP12 and an HA tag were fused to the C terminus of the endogenous Rpl13a using the "pop-in/pop-out" strategy and confirmed by sequencing. Expression was assessed by Western blot using α-HA antibodies. Rapamycin binds to FKBP12, creating an interaction surface for the FKBP12-rapamycin–binding (FRB) domain for human mammalian target of rapamycin (Chen et al., 1995). We generated a *BEM1-2xFRB-HA*-GFP construct and integrated it at the *BEM1* locus, with correct integration confirmed by sequencing. Expression was checked by Western blot and microscopy.

Cdc42 purification

GST-Cdc42 was expressed in *Escherichia coli* BL21(DE3) as described elsewhere (Bose et al., 2001). Cell pellets were resuspended in sonication buffer (50 mM phosphate buffer, pH 7.6, 1 mM EDTA, 150 mM NaCl, 1 mM DTT, 10% glycerol, 5 µm GDP, and 1x protease inhibitor cocktail [Complete, EDTA-free tablet; Roche]) and then disrupted by sonication. Lysates were clarified by centrifugation at 10,000 *g* for 15 min at 4°C and incubated for 2 h with Glutathione Sepharose 4B (GE Healthcare) at 4°C. Beads were washed twice in sonication buffer containing 1 mM glutathione, and GST-Cdc42 was purified in sonication buffer containing 10 mM glutathione. The eluate was dialyzed against dialysis buffer (20 mM Tris, 5 mM $MgCl_2$, 1 mM EDTA, 5 µM GDP, 2 mM DTT, and 50% glycerol) overnight at 4°C.

Immunoprecipitation and GEF assay

Yeast lysates were prepared by high-speed vortexing with glass beads in lysis buffer (20 mM Tris, pH 7.6, 150 mM NaCl, 1 mM EDTA, 5% glycerol, 0.5% NP-40, 4 mM β-glycerophosphate, 4 mM NaF, 4 mM Na_3VO_4, 4 mM $Na_4P_2O_7$, 2 mM DTT, and 1x protease inhibitor cocktail). Lysates were clarified by centrifugation at 10,000 *g* for 10 min at 4°C. For immunoprecipitation, 10-µl antibody-coupled beads (monoclonal anti-HA agarose, Sigma-Aldrich) were mixed with lysate containing 2.5 mg protein that was diluted to 1 ml using lysis buffer without NP-40. After incubation at 4°C for 2 h, beads were pelleted and washed twice with lysis buffer and once with GEF buffer (20 mM Tris, 5 mM $MgCl_2$, 1 mM EDTA, 5 µM GDP, and 2 mM DTT). Beads were then incubated with 40 pmol GST-Cdc42 and 2.5 µCi GTP-γ-^{35}S in 45 µl GEF buffer for 15 min at RT, with gentle mixing every 3 min. Reactions were stopped with 0.5 ml ice-cold GEF buffer, after which beads were pelleted by centrifugation and supernatants were filtered through nitrocellulose filters (Protran BA 85, Whatman; GE Healthcare) to trap and assay protein-bound radioactivity. The beads containing immunoprecipitated protein were then incubated with SDS sample buffer (2% SDS, 2 mM β-mercaptoethanol, 4% glycerol, 40 mM Tris-HCl, pH 6.8, and 0.01% bromophenol blue) at 95°C, and Cdc24 levels were analyzed by immunoblot.

Spot assay

For cell viability analysis, cells were grown overnight in yeast extract Bacto peptone (YEP; 2% Bacto peptone, 1% yeast extract, 0.001% uracil and adenine) medium (BD Biosciences) with 2% dextrose (dex) liquid media and diluted to ∼3×10^6 cells/ml^{-1}. 10-fold serial dilutions (10^4, 10^3,10^2, and 10 cells) were spotted onto YEP + dex agar plates or complete synthetic medium (CSM; MP Biomedicals) + dex agar plates lacking uracil. For cell viability analysis on 5-fluoroorotic acid + dex agar plates, cells were diluted 2×10^7 cells/ml^{-1} and spotted in 10-fold serial dilutions starting from 10^5 cells. To assess the effects of overexpression of MT-Cdc24 or MT-Cdc24 and Bem1, cells were grown to mid-log phase in YEP + dex liquid media at 24°C and spotted in 10-fold serial dilutions starting from 6,000 cells onto YEP + dex agar plates containing the indicated concentrations of β-estradiol. β-Estradiol (Sigma-Aldrich) was stored as a 10-mM stock in 100% ethanol. Because of variations in β-estradiol stocks and YEP + dex plate volume and age, indicated β-estradiol concentrations are approximate.

Immunoblotting

For Western blot analysis, $1–2 \times 10^7$ cells were collected from log phase cultures for total protein extraction by TCA precipitation as described previously (Keaton et al., 2008). Electrophoresis and Western blotting were performed as described previously (Bose et al., 2001). Monoclonal mouse anti-GFP antibodies (Roche) were used at 1:500 dilution. Rabbit polyclonal anti-Cdc11 antibodies (Santa Cruz Biotechnology, Inc.) were used at 1:5,000 dilution. Fluorophore-conjugated secondary antibodies against mouse (IRDye800 conjugated goat anti–mouse IgG; Rockland Immunochemicals) or antibodies against rabbit (Alexa Fluor 680 goat anti–rabbit IgG, Invitrogen) were used at 1:5,000 dilution. Blots were visualized by the ODYSSEY imaging system (LI-COR Biosciences).

Microscopy and image analysis

Before imaging, cells were grown CSM + dex to mid-log phase. Cells were mounted onto a CSM + dex slab solidified with 2% aga-

rose (Denville Scientific Inc.), and sealed with petroleum jelly. Cells were imaged at 24°C unless otherwise noted. Also unless otherwise noted, images were acquired by using an Andor Revolution XD spinning-disk confocal microscope (Olympus) with a Yokogawa CSU-X1 5,000 rpm disc unit, 100×/1.4 UPlanSApo oil-immersion objective, and were captured with an Andor Ixon3 897 512 EM charge-coupled device (CCD) camera using MetaMorph software (Universal Imaging). 525-nm ± single-band filters (Olympus) were used for GFP fluorescence, and EdgeBasic Long Pass 568-nm filters (Semrock) were used for mCherry fluorescence. Images were captured by 200-ms exposure to the diode laser at 15% maximal output in z-stacks of 17 planes with 0.5-µm spacing unless otherwise noted. An EM gain setting of 200 was used for the EM CCD camera.

Differential interference contrast (DIC) images and time lapses were, unless otherwise noted, acquired with a Z1 motorized Zeiss Axio Observer microscope (Carl Zeiss) with a 100×/1.46 oil Plan Apochromat DIC WD objective and a QuantEM backthinned EMCCD camera (Photometrics) with a 100-ms exposure and EM gain set to 200 using MetaMorph software.

Scanning confocal images were acquired with a Zeiss 780 confocal microscope with an Argon/2 and 561nm diode laser, a 63×/1.4 oil Plan Apochromat 44 07 62 WD 0.19 mm objective, and were captured with a GaAsP high QE 32 channel spectral array detector. For image acquisition, we used Zen 2010 software (Carl Zeiss). Representative cells were compiled to a single image for presentation using ImageJ (Fiji) and Illustrator (Adobe).

Hydroxyurea treatment

To examine polarization dynamics of Bem1 and Bem1^{N253D}, we enriched for G1 cells that are about to polarize by hydroxyurea arrest-release synchronization as previously described (Howell et al., 2012). Cells were grown to mid-log phase in CSM + dex at 30°C and arrested with 200 mM HU (Sigma-Aldrich) for 3 h, washed, released into fresh media for 1 h, harvested, and mounted for live cell microscopy. Images were captured in z-stacks of 30 planes with 0.24-µm spacing, using 10% maximal fluorescent light. Images were deconvolved using Hyugens Essential software (Scientific Volume Imaging). The classic maximum-likelihood estimation and predicted point spread function method with signal-to-noise ratio of 3 was used with a constant background across all images from the same channel on the same day. The output format was 16-bit, unscaled images to enable comparison of pixel values. Quantification of Bem1-GFP intensities used Volocity (Improvision; Howell et al., 2012). A threshold was set that would highlight only the polarized signal, and the summed polarized intensity was recorded. Changes in intensity are reported as a percentage of maximum summed intensity for that cell.

Rapamycin treatment

Cells were grown in CSM + dex to mid-log phase at 24°C before rapamycin treatment. For images in rapamycin, cells were mounted on CSM + dex agarose slabs with 50 µg/ml rapamycin (or DMSO for controls) and imaged.

β-Estradiol treatment

Cells were grown in CSM + dex to mid-log phase at 24°C and resuspended in fresh media containing the indicated concentration of β-estradiol. Cells were then incubated at 24°C for 4 h, harvested, and mounted onto CSM + dex agarose slabs and imaged.

Online supplemental material

Fig. S1 shows additional examples of cells depicted in Fig. 1 B. Fig. S2 shows the results of sequestering Bem1 in the cytoplasm in *RSR1* cells. Fig. S3 shows control experiments for Fig. 3 with phosphorylatable MT-Cdc24 and MT-Cdc24$^{\Delta PB1}$. Fig. S3 also shows representative *rsr1*Δ *bem1*Δ cells rescued by Cdc24^{38A}-GFP-Snc2 or Cdc24$^{37A\ \Delta PB1}$-GFP-Snc2. Video 1 shows the results of sequestering Bem1 in the cytoplasm in *rsr1*Δ cells. Video 2 shows the results of sequestering Bem1 in the cytoplasm in *rsr1*Δ cells expressing additional Bem1 targeted to the plasma membrane (Bem1-GFP-Snc2^{V39A,M42A}). Video 3 shows *cdc24-1* cells expressing MT-Cdc24$^{37A\ \Delta PB1}$ shifted to restrictive temperature. Table S1 shows yeast strains used in this study. Online supplemental material is available at http://www.jcb.org/cgi/content/full/jcb.201506108/DC1.

Acknowledgments

We thank S. Smith and R. Li for providing strains. We also thank N. Savage, N. Buchler, P. Brennwald, T. Elston, and members of the Lew laboratory for stimulating discussions and comments on the manuscript.

This work was supported by National Institutes of Health/National Institute of General Medical Sciences grant GM62300 to D.J. Lew.

The authors declare no competing financial interests.

Submitted: 22 June 2015
Accepted: 1 September 2015

References

Bendezú, F.O., V. Vincenzetti, D. Vavylonis, R. Wyss, H. Vogel, and S.G. Martin. 2015. Spontaneous Cdc42 polarization independent of GDI-mediated extraction and actin-based trafficking. *PLoS Biol.* 13:e1002097.

Bose, I., J.E. Irazoqui, J.J. Moskow, E.S. Bardes, T.R. Zyla, and D.J. Lew. 2001. Assembly of scaffold-mediated complexes containing Cdc42p, the exchange factor Cdc24p, and the effector Cla4p required for cell cycle-regulated phosphorylation of Cdc24p. *J. Biol. Chem.* 276:7176–7186. http://dx.doi.org/10.1074/jbc.M010546200

Chen, H., C.C. Kuo, H. Kang, A.S. Howell, T.R. Zyla, M. Jin, and D.J. Lew. 2012. Cdc42p regulation of the yeast formin Bni1p mediated by the effector Gic2p. *Mol. Biol. Cell.* 23:3814–3826. http://dx.doi.org/10.1091/mbc.E12-05-0400

Chen, J., X.F. Zheng, E.J. Brown, and S.L. Schreiber. 1995. Identification of an 11-kDa FKBP12-rapamycin-binding domain within the 289-kDa FKBP12-rapamycin-associated protein and characterization of a critical serine residue. *Proc. Natl. Acad. Sci. USA.* 92:4947–4951. http://dx.doi.org/10.1073/pnas.92.11.4947

Etienne-Manneville, S. 2004. Cdc42—the centre of polarity. *J. Cell Sci.* 117:1291–1300. http://dx.doi.org/10.1242/jcs.01115

Gietz, R.D., and A. Sugino. 1988. New yeast-*Escherichia coli* shuttle vectors constructed with in vitro mutagenized yeast genes lacking six-base pair restriction sites. *Gene.* 74:527–534. http://dx.doi.org/10.1016/0378-1119(88)90185-0

Goryachev, A.B., and A.V. Pokhilko. 2008. Dynamics of Cdc42 network embodies a Turing-type mechanism of yeast cell polarity. *FEBS Lett.* 582:1437–1443. http://dx.doi.org/10.1016/j.febslet.2008.03.029

Gulli, M.P., M. Jaquenoud, Y. Shimada, G. Niederhäuser, P. Wiget, and M. Peter. 2000. Phosphorylation of the Cdc42 exchange factor Cdc24 by the PAK-like kinase Cla4 may regulate polarized growth in yeast. *Mol. Cell.* 6:1155–1167. http://dx.doi.org/10.1016/S1097-2765(00)00113-1

Haruki, H., J. Nishikawa, and U.K. Laemmli. 2008. The anchor-away technique: rapid, conditional establishment of yeast mutant phenotypes. *Mol. Cell.* 31:925–932. http://dx.doi.org/10.1016/j.molcel.2008.07.020

Howell, A.S., and D.J. Lew. 2012. Morphogenesis and the cell cycle. *Genetics.* 190:51–77. http://dx.doi.org/10.1534/genetics.111.128314

Howell, A.S., N.S. Savage, S.A. Johnson, I. Bose, A.W. Wagner, T.R. Zyla, H.F. Nijhout, M.C. Reed, A.B. Goryachev, and D.J. Lew. 2009. Singularity in polarization: rewiring yeast cells to make two buds. *Cell.* 139:731–743. http://dx.doi.org/10.1016/j.cell.2009.10.024

Howell, A.S., M. Jin, C.F. Wu, T.R. Zyla, T.C. Elston, and D.J. Lew. 2012. Negative feedback enhances robustness in the yeast polarity establishment circuit. *Cell.* 149:322–333. http://dx.doi.org/10.1016/j.cell.2012.03.012

Irazoqui, J.E., A.S. Gladfelter, and D.J. Lew. 2003. Scaffold-mediated symmetry breaking by Cdc42p. *Nat. Cell Biol.* 5:1062–1070. http://dx.doi.org/10.1038/ncb1068

Ito, T., Y. Matsui, T. Ago, K. Ota, and H. Sumimoto. 2001. Novel modular domain PB1 recognizes PC motif to mediate functional protein-protein interactions. *EMBO J.* 20:3938–3946. http://dx.doi.org/10.1093/emboj/20.15.3938

Johnson, J.L., J.W. Erickson, and R.A. Cerione. 2009. New insights into how the Rho guanine nucleotide dissociation inhibitor regulates the interaction of Cdc42 with membranes. *J. Biol. Chem.* 284:23860–23871. http://dx.doi.org/10.1074/jbc.M109.031815

Johnson, J.M., M. Jin, and D.J. Lew. 2011. Symmetry breaking and the establishment of cell polarity in budding yeast. *Curr. Opin. Genet. Dev.* 21:740–746. http://dx.doi.org/10.1016/j.gde.2011.09.007

Jost, A.P., and O.D. Weiner. 2015. Probing yeast polarity with acute, reversible, optogenetic inhibition of protein function. *ACS Synth. Biol*. http://dx.doi.org/10.1021/acssynbio.5b00053

Keaton, M.A., L. Szkotnicki, A.R. Marquitz, J. Harrison, T.R. Zyla, and D.J. Lew. 2008. Nucleocytoplasmic trafficking of G2/M regulators in yeast. *Mol. Biol. Cell.* 19:4006–4018. http://dx.doi.org/10.1091/mbc.E08-03-0286

Kozubowski, L., K. Saito, J.M. Johnson, A.S. Howell, T.R. Zyla, and D.J. Lew. 2008. Symmetry-breaking polarization driven by a Cdc42p GEF-PAK complex. *Curr. Biol.* 18:1719–1726. http://dx.doi.org/10.1016/j.cub.2008.09.060

Kuo, C.C., N.S. Savage, H. Chen, C.F. Wu, T.R. Zyla, and D.J. Lew. 2014. Inhibitory GEF phosphorylation provides negative feedback in the yeast polarity circuit. *Curr. Biol.* 24:753–759. http://dx.doi.org/10.1016/j.cub.2014.02.024

Layton, A.T., N.S. Savage, A.S. Howell, S.Y. Carroll, D.G. Drubin, and D.J. Lew. 2011. Modeling vesicle traffic reveals unexpected consequences for Cdc42p-mediated polarity establishment. *Curr. Biol.* 21:184–194. http://dx.doi.org/10.1016/j.cub.2011.01.012

Longtine, M.S., A. McKenzie III, D.J. Demarini, N.G. Shah, A. Wach, A. Brachat, P. Philippsen, and J.R. Pringle. 1998. Additional modules for versatile and economical PCR-based gene deletion and modification in *Saccharomyces cerevisiae. Yeast.* 14:953–961. http://dx.doi.org/10.1002/(SICI)1097-0061(199807)14:10<953::AID-YEA293>3.0.CO;2-U

Nern, A., and R.A. Arkowitz. 1999. A Cdc24p-Far1p-Gbetagamma protein complex required for yeast orientation during mating. *J. Cell Biol.* 144:1187–1202. http://dx.doi.org/10.1083/jcb.144.6.1187

Park, H.O., and E. Bi. 2007. Central roles of small GTPases in the development of cell polarity in yeast and beyond. *Microbiol. Mol. Biol. Rev.* 71:48–96. http://dx.doi.org/10.1128/MMBR.00028-06

Savage, N.S., A.T. Layton, and D.J. Lew. 2012. Mechanistic mathematical model of polarity in yeast. *Mol. Biol. Cell.* 23:1998–2013. http://dx.doi.org/10.1091/mbc.E11-10-0837

Shimada, Y., P. Wiget, M.P. Gulli, E. Bi, and M. Peter. 2004. The nucleotide exchange factor Cdc24p may be regulated by auto-inhibition. *EMBO J.* 23:1051–1062. http://dx.doi.org/10.1038/sj.emboj.7600124

Siniossoglou, S., E.C. Hurt, and H.R. Pelham. 2000. Psr1p/Psr2p, two plasma membrane phosphatases with an essential DXDX(T/V) motif required for sodium stress response in yeast. *J. Biol. Chem.* 275:19352–19360. http://dx.doi.org/10.1074/jbc.M001314200

Slaughter, B.D., A. Das, J.W. Schwartz, B. Rubinstein, and R. Li. 2009. Dual modes of cdc42 recycling fine-tune polarized morphogenesis. *Dev. Cell.* 17:823–835. http://dx.doi.org/10.1016/j.devcel.2009.10.022

Slaughter, B.D., J.R. Unruh, A. Das, S.E. Smith, B. Rubinstein, and R. Li. 2013. Non-uniform membrane diffusion enables steady-state cell polarization via vesicular trafficking. *Nat. Commun.* 4:1380. http://dx.doi.org/10.1038/ncomms2370

Smith, S.E., B. Rubinstein, I. Mendes Pinto, B.D. Slaughter, J.R. Unruh, and R. Li. 2013. Independence of symmetry breaking on Bem1-mediated autocatalytic activation of Cdc42. *J. Cell Biol.* 202:1091–1106. http://dx.doi.org/10.1083/jcb.201304180

Takahashi, S., and P.M. Pryciak. 2008. Membrane localization of scaffold proteins promotes graded signaling in the yeast MAP kinase cascade. *Curr. Biol.* 18:1184–1191. http://dx.doi.org/10.1016/j.cub.2008.07.050

Toenjes, K.A., M.M. Sawyer, and D.I. Johnson. 1999. The guanine-nucleotide-exchange factor Cdc24p is targeted to the nucleus and polarized growth sites. *Curr. Biol.* 9:1183–1186, S1. http://dx.doi.org/10.1016/S0960-9822(00)80022-6

Valdez-Taubas, J., and H.R. Pelham. 2003. Slow diffusion of proteins in the yeast plasma membrane allows polarity to be maintained by endocytic cycling. *Curr. Biol.* 13:1636–1640. http://dx.doi.org/10.1016/j.cub.2003.09.001

Watson, L.J., G. Rossi, and P. Brennwald. 2014. Quantitative analysis of membrane trafficking in regulation of Cdc42 polarity. *Traffic.* 15:1330–1343. http://dx.doi.org/10.1111/tra.12211

Wedlich-Soldner, R., S. Altschuler, L. Wu, and R. Li. 2003. Spontaneous cell polarization through actomyosin-based delivery of the Cdc42 GTPase. *Science.* 299:1231–1235. http://dx.doi.org/10.1126/science.1080944

Wu, C.F., N.S. Savage, and D.J. Lew. 2013. Interaction between bud-site selection and polarity-establishment machineries in budding yeast. *Philos. Trans. R. Soc. Lond. B Biol. Sci.* 368:20130006. http://dx.doi.org/10.1098/rstb.2013.0006

Ziman, M., D. Preuss, J. Mulholland, J.M. O'Brien, D. Botstein, and D.I. Johnson. 1993. Subcellular localization of Cdc42p, a *Saccharomyces cerevisiae* GTP-binding protein involved in the control of cell polarity. *Mol. Biol. Cell.* 4:1307–1316. http://dx.doi.org/10.1091/mbc.4.12.1307